Analytical approaches for large-scale structures in some modified-gravity scenarios

P. Valageas

IPhT - CEA Saclay

coll. with A. Barreira, Ph. Brax, S. Clesse, B. Li, L. Rizzo.

Paris - May 2016

- Modified gravity models

- Perturbative approach (SPT)

- Spherical collapse

- Matter power spectrum (SPT+halo model)

- Density probability distribution

- Conclusion

Accelerated expansion of the Universe → - dark energy

- modified gravity

Most of the models involve one or more scalar fields, which experience self-interactions and may also interact with matter.

→ "Fifth force" that has not been seen in local gravity experiments !

- the scalar field does not interact with baryonic matter components

- there is a mechanism to suppress the fifth force in local environments

→ "Screening" mechanisms associated with non-linearities of the system.

Definitions of some models

a) f(R) models

Add a function of the Ricci scalar, f(R), to the Einstein-Hilbert action:

$$S = \int d^4x \, \sqrt{-g} \left[\frac{M_{\rm Pl}^2}{2} (R + f(R)) + \mathcal{L}_m \right]$$

$$f(R) = -2\Lambda - \frac{f_{R_0} c^2}{n} \frac{R_0^{n+1}}{R^n}$$

$n = 1, \quad |f_{R_0}| \leq 10^{-5}$ Solar System constraints

Modified Poisson equation: $$\boxed{\nabla^2 \Psi = \frac{16\pi \mathcal{G}}{3} a^2 \delta\rho - \frac{a^2}{6} \delta R}$$

Constraint equation: $$\nabla^2 \delta f_R = \frac{a^2}{3} [\delta R - 8\pi \mathcal{G} \delta\rho]$$

$$f_R = \frac{df}{dR} = f_{R_0} c^2 \frac{R_0^{n+1}}{R^{n+1}}$$

(quasi-static approximation)

b) Scalar field models

Dilaton models or symmetron models

Scalar-tensor theories $$S = \int d^4x \, \sqrt{-g} \left[\frac{M_{\rm Pl}^2}{2} R - \frac{1}{2} (\nabla\varphi)^2 - V(\varphi) \right] + \int d^4x \, \sqrt{-\tilde{g}} \, \mathcal{L}_m(\psi_m, \tilde{g}_{\mu\nu})$$

$$\tilde{g}_{\mu\nu} = A(\varphi)^2 \, g_{\mu\nu}$$

Jordan-frame metric

Einstein-frame metric

Modified Poisson equation (5th force): $\Psi = \Psi_N + \Psi_A$

$$\nabla^2 \Psi_N = 4\pi \mathcal{G} a^2 \delta\rho \qquad \Psi_A = c^2 (A - \bar{A}) \qquad (A \simeq 1)$$

Klein-Gordon eq.: $$\frac{c^2}{a^2} \nabla^2 \varphi = \frac{dV}{d\varphi} + \rho \frac{dA}{d\varphi}$$

(quasi-static approximation)

Perturbative approach

1) Use the quasi-static approximation, which applies to small scales dominated by spatial gradients

→ Obtain a non-linear equation that relates the new field to the matter density

$$\mathcal{F}(\delta R, \delta\rho) = 0 \qquad\qquad \mathcal{F}(\delta\varphi, \delta\rho) = 0$$

This allows one to eventually go back to the standard LCDM formalism (i.e., we can eliminate the new degree of freedom).

2) Solve this equation through a perturbative expansion over the nonlinear density fluctuation

$$\delta\tilde{R}(\mathbf{k}) = \sum_{n=1}^{\infty} \int d\mathbf{k}_1 ... d\mathbf{k}_n \; \delta_D(\mathbf{k}_1 + ... + \mathbf{k}_n) \; h_n(\mathbf{k}_1, ..., \mathbf{k}_n) \; \delta\tilde{\rho}(\mathbf{k}_1) ... \delta\tilde{\rho}(\mathbf{k}_n)$$

$$\delta\tilde{\varphi}(\mathbf{k}) = \sum_{n=1}^{\infty} \int d\mathbf{k}_1 ... d\mathbf{k}_n \; \delta_D(\mathbf{k}_1 + ... + \mathbf{k}_n) \; h_n(\mathbf{k}_1, ..., \mathbf{k}_n) \; \delta\tilde{\rho}(\mathbf{k}_1) ... \delta\tilde{\rho}(\mathbf{k}_n)$$

3) Obtain the expression of the full "gravitational" potential (Newton+5th force)

$$\tilde{\Psi}(\mathbf{k}) = \sum_{n=1}^{\infty} \int d\mathbf{k}_1 ... d\mathbf{k}_n \; \delta_D(\mathbf{k}_1 + ... + \mathbf{k}_n) \; H_n(\mathbf{k}_1, ..., \mathbf{k}_n) \; \delta\tilde{\rho}(\mathbf{k}_1) ... \delta\tilde{\rho}(\mathbf{k}_n)$$

a) f(R) models

- **Constraint equation:** $$\nabla^2 \delta f_R = \frac{a^2}{3}[\delta R - 8\pi\mathcal{G}\delta\rho]$$

$$n \geq 1: \quad \kappa_n(a) = H^{2n-2}\frac{d^n f_R}{dR^n}(\bar{R})$$

$$\left(1 - \frac{\nabla^2}{a^2 m^2}\right)\cdot \delta R = \frac{\delta\rho}{M_{\rm Pl}^2} + \sum_{n=2}^{\infty}\frac{3H^{2-2n}\kappa_n}{a^2 n!}\nabla^2(\delta R)^n$$

- **Modified Poisson equation:** $$\nabla^2\Psi = \frac{16\pi\mathcal{G}}{3}a^2\delta\rho - \frac{a^2}{6}\delta R \quad \Rightarrow \quad \Psi(\delta\rho)$$

b) Scalar field models (Dilaton or symmetrons)

- **Klein-Gordon eq.:** $$\frac{c^2}{a^2}\nabla^2\varphi = \frac{dV}{d\varphi} + \rho\frac{dA}{d\varphi}$$

$$n \geq 1: \quad \beta_n(a) = M_{\rm Pl}^n \frac{d^n A}{d\varphi^n}(\bar{\varphi})$$

$$n \geq 2: \quad \kappa_n(a) = \frac{M_{\rm Pl}^{n-2}}{c^2}\left[\frac{d^n V}{d\varphi^n}(\bar{\varphi}) + \bar{\rho}\frac{d^n A}{d\varphi^n}(\bar{\varphi})\right]$$

$$\left(\frac{\nabla^2}{a^2} - m^2\right)\cdot\delta\varphi = \frac{\beta\,\delta\rho}{c^2 M_{\rm Pl}} + \frac{\beta_2\,\delta\rho}{c^2 M_{\rm Pl}^2}\delta\varphi + \sum_{n=2}^{\infty}\left(\frac{\kappa_{n+1}}{M_{\rm Pl}^{n-1}} + \frac{\beta_{n+1}\delta\rho}{c^2 M_{\rm Pl}^{n+1}}\right)\frac{(\delta\varphi)^n}{n!}$$

- **Modified Poisson equation (5th force):** $$\Psi = \Psi_N + \Psi_A \qquad \Psi_A = c^2(A - \bar{A})$$

$$\Psi_A = \sum_{n=1}^{\infty}\frac{c^2\beta_n}{M_{\rm Pl}^n n!}(\delta\varphi)^n \quad \Rightarrow \quad \Psi(\delta\rho)$$

4) Write the equations of motion (in the single-stream approx.), with the ``new gravitational potential''

Continuity eq.: $$\frac{\partial \delta}{\partial \tau} + \nabla \cdot [(1+\delta)\mathbf{v}] = 0$$

Euler eq.: $$\frac{\partial \mathbf{v}}{\partial \tau} + (\mathbf{v}\cdot\nabla)\mathbf{v} + \mathcal{H}\mathbf{v} = -\nabla\Psi$$

5th force

(K-mouflage models)

$$\frac{\partial \mathbf{v}}{\partial \tau} + (\mathbf{v}\cdot\nabla)\mathbf{v} + \left(\mathcal{H} + \frac{d\ln\bar{A}}{d\tau}\right)\mathbf{v} = -\nabla\Psi$$

friction

5th force

This can be written in a more concise form as: $$\mathcal{O}(x,x')\cdot\tilde{\psi}(x') = \sum_{n=2}^{\infty} K_n^s(x;x_1,..,x_n)\cdot\tilde{\psi}(x_1)...\tilde{\psi}(x_n)$$

2-component vector: $$\psi = \begin{pmatrix} \delta \\ -(\nabla\cdot\mathbf{v})/\dot{a} \end{pmatrix}$$

time coordinate: $\eta = \ln(a)$

$x = (\mathbf{k}, \eta, i)$

Linear part: $$\mathcal{O}(x,x') = \delta_D(\eta'-\eta)\,\delta_D(\mathbf{k}'-\mathbf{k}) \begin{pmatrix} \frac{\partial}{\partial\eta} & -1 \\ -\frac{3}{2}\Omega_m(1+\epsilon_1) & \frac{\partial}{\partial\eta} + \frac{1-3w_\varphi^{\mathrm{eff}}\Omega_\varphi^{\mathrm{eff}}}{2} + \epsilon_2 \end{pmatrix}$$

modified-gravity impact at linear order

Equal-time kernels: $$K_n^s = \delta_D(\eta_1-\eta)...\delta_D(\eta_n-\eta)\delta_D(\mathbf{k}_1+...+\mathbf{k}_n)\gamma^s_{i;i_1,..,i_n}(\mathbf{k}_1,..,\mathbf{k}_n;\eta)$$

new time and scale dependence

5) Linear theory

★ f(R) and dilaton models:

$$\frac{\partial^2 D}{\partial \eta^2} + \frac{1-3w\Omega_{\rm de}}{2}\frac{\partial D}{\partial \eta} - \frac{3}{2}\Omega_m [1+\epsilon(k,\eta)] D = 0$$

scale-dependence of the linear modes
(scale and time dependent
effective Newton constant)

★ K-mouflage models:

$$\frac{d^2 D}{d\eta^2} + \left(\frac{1-3w_\varphi^{\rm eff}\Omega_\varphi^{\rm eff}}{2} + \epsilon_2\right)\frac{dD}{d\eta} - \frac{3}{2}\Omega_m (1+\epsilon_1) D = 0$$

scale-independent modified
linear growing mode

★ $f(R): \quad \epsilon(k,\eta) = \dfrac{k^2}{3(a^2m^2+k^2)}$

scalar field models: $\epsilon(k,\eta) = \dfrac{2\beta^2 k^2}{a^2m^2+k^2}$

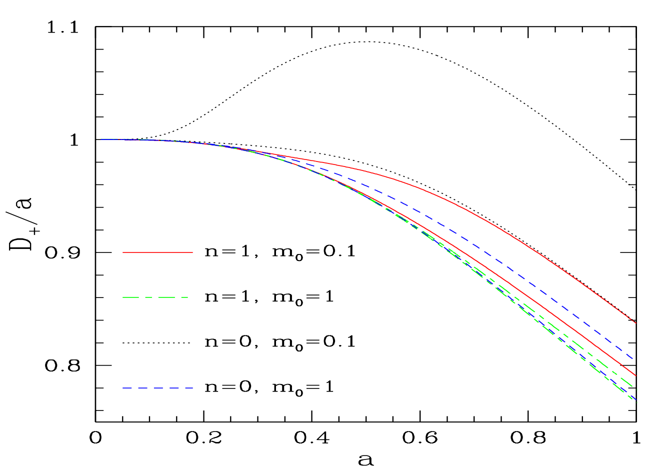

FIG. 1: Linear growing mode $D_+(k,t)$ normalized to the scale factor $a(t)$ for four (n,m_0) models. In each case we show the results for wavenumbers $k = 1h\mathrm{Mpc}^{-1}$ (lower curve) and $k = 5h\mathrm{Mpc}^{-1}$ (upper curve), as a function of $a(t)$. These two scales are in the non-linear regime and have only been chosen to exemplify the type of effects obtained in modified gravity.

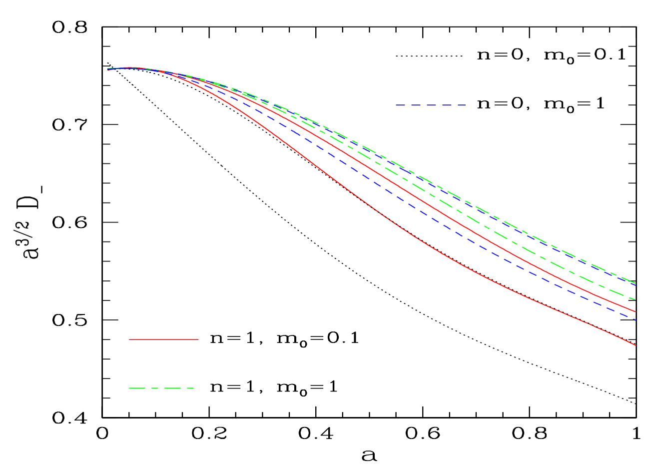

FIG. 2: Linear decaying mode $D_-(k,t)$ normalized to $a(t)^{-3/2}$ for four (n,m_0) models. In each case we show the results for wavenumbers $k = 1h\mathrm{Mpc}^{-1}$ (upper curve) and $5h\mathrm{Mpc}^{-1}$ (lower curve), as a function of $a(t)$. These two scales are in the non-linear regime and have only been chosen to exemplify the type of effects obtained in modified gravity.

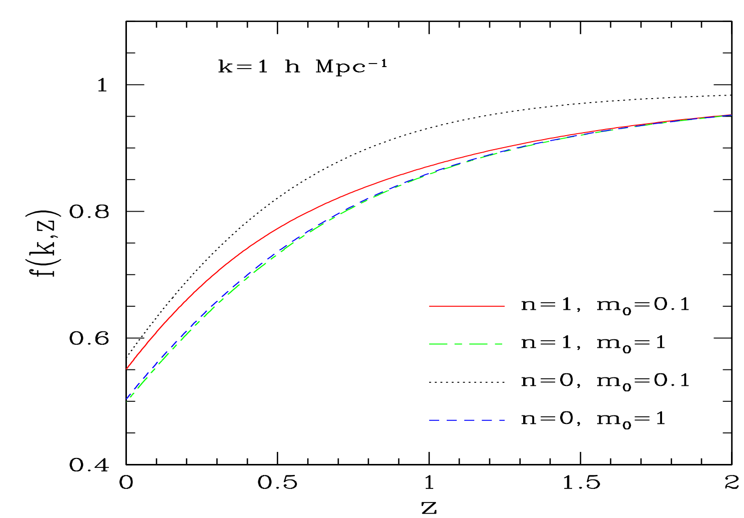

FIG. 5: Linear growth rate $f(k,z) = \partial \ln D_+/\partial \ln a$ for wavenumber $k = 1h\mathrm{Mpc}^{-1}$, for four (n,m_0) models.

Linear growing mode as
a function of time

Linear decaying mode as
a function of time

Linear growth rate as
a function of time

6) One-loop power spectrum

As in the LCDM case, we can write the solution of the equation of motion as a perturbative expansion over powers of the linear growing mode:

$$\tilde{\psi}(x) = \sum_{n=1}^{\infty} \tilde{\psi}^{(n)}(x), \quad \text{with} \quad \tilde{\psi}^{(n)} \propto (\tilde{\psi}_L)^n$$

Diagrams:

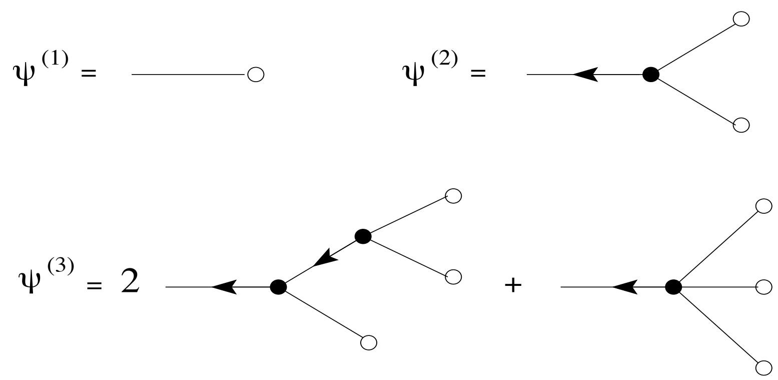

- white circles: linear solution
- black dots: vertices
- lines with an arrow: retarded propagator

new cubic vertex

This gives in turns the density 2-pt correlation function, or the density power spectrum:

$$P(k) = P_{\text{tree}}(k) + P_{\text{1loop}}(k) + \ldots \qquad P_{\text{tree}} = P_L \qquad P_{\text{1loop}} = P_{22} + P_{31} + P_{31}^{\Psi}$$

Diagrams:

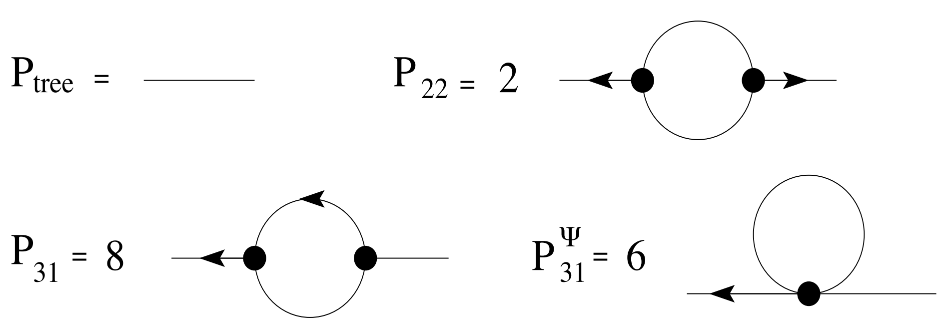

new diagram

Relative deviations from LCDM for the power spectrum P(k)

a) f(R) models

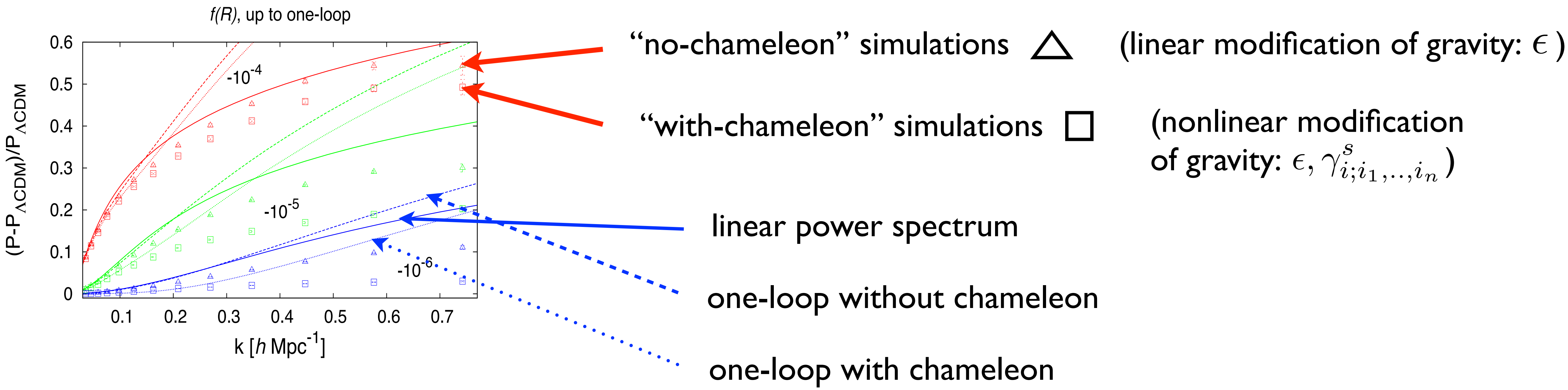

FIG. 3: Relative deviation from Λ-CDM of the power spectrum in $f(R)$ theories, at redshift $z = 0$, for $n = 1$ and $f_{R_0} = -10^{-4}, -10^{-5}$, and -10^{-6}. In each case, the triangles and the squares are the results of the "no-chameleon" and "with-chameleon" simulations from [25], respectively. We plot the relative deviation of the linear power (solid line), of the one-loop power without "chameleon" effect ($\gamma^s_{2;1,1} = \gamma^s_{2;1,1,1} = 0$) (dashed line), and with lowest-order "chameleon" effect ($\gamma^s_{2;1,1} \neq 0$, $\gamma^s_{2;1,1,1} = 0$) (dotted line).

- ✦ Including the quadratic vertex $\gamma^s_{2;1,1}$ gives the first sign of the chameleon effect.
- ✦ The cubic vertex makes no significant change.
- ✦ Going to 1-loop does not increase much the range of scales.

b) Scalar field models

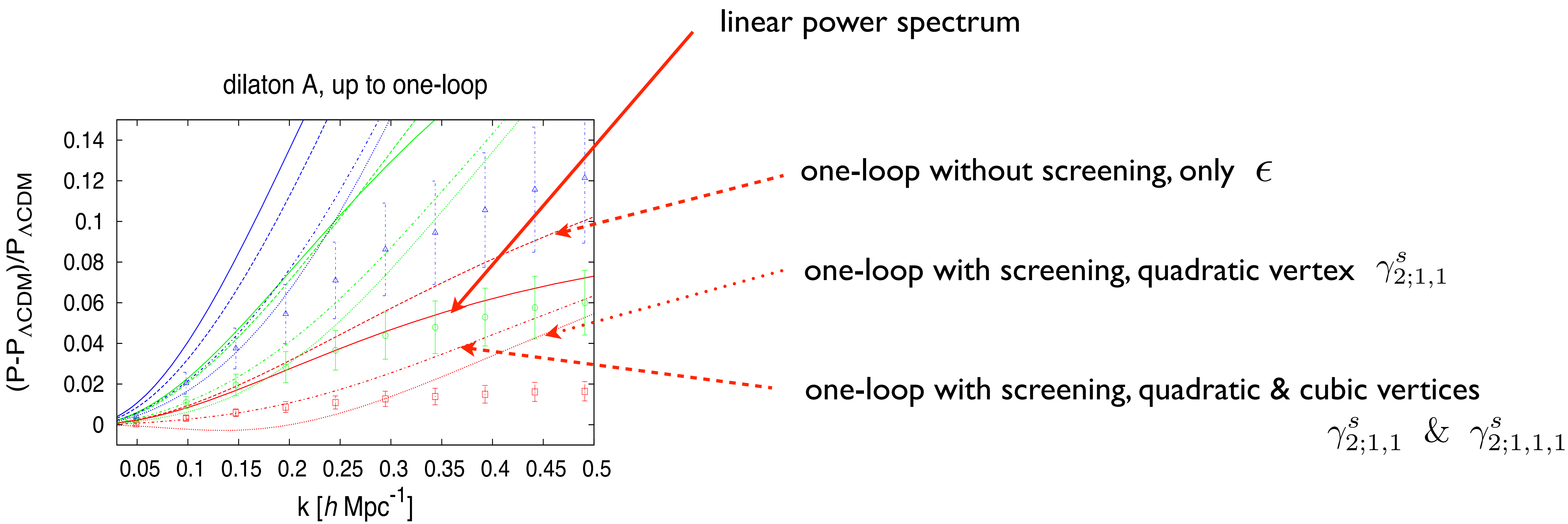

✦ Including the quadratic vertex gives the first sign of the screening effect.

✦ This can "over-correct" the deviation from LCDM and give a power spectrum that is smaller than the LCDM one. (The linear term speeds up the collapse, but the quadratic term slows down and would halt the collapse before reaching high densities.)

✦ The cubic vertex corrects for the "over-screening".

⟹ gradual convergence of higher orders on perturbative scales

✦ Going to 1-loop increases somewhat the range of scales.

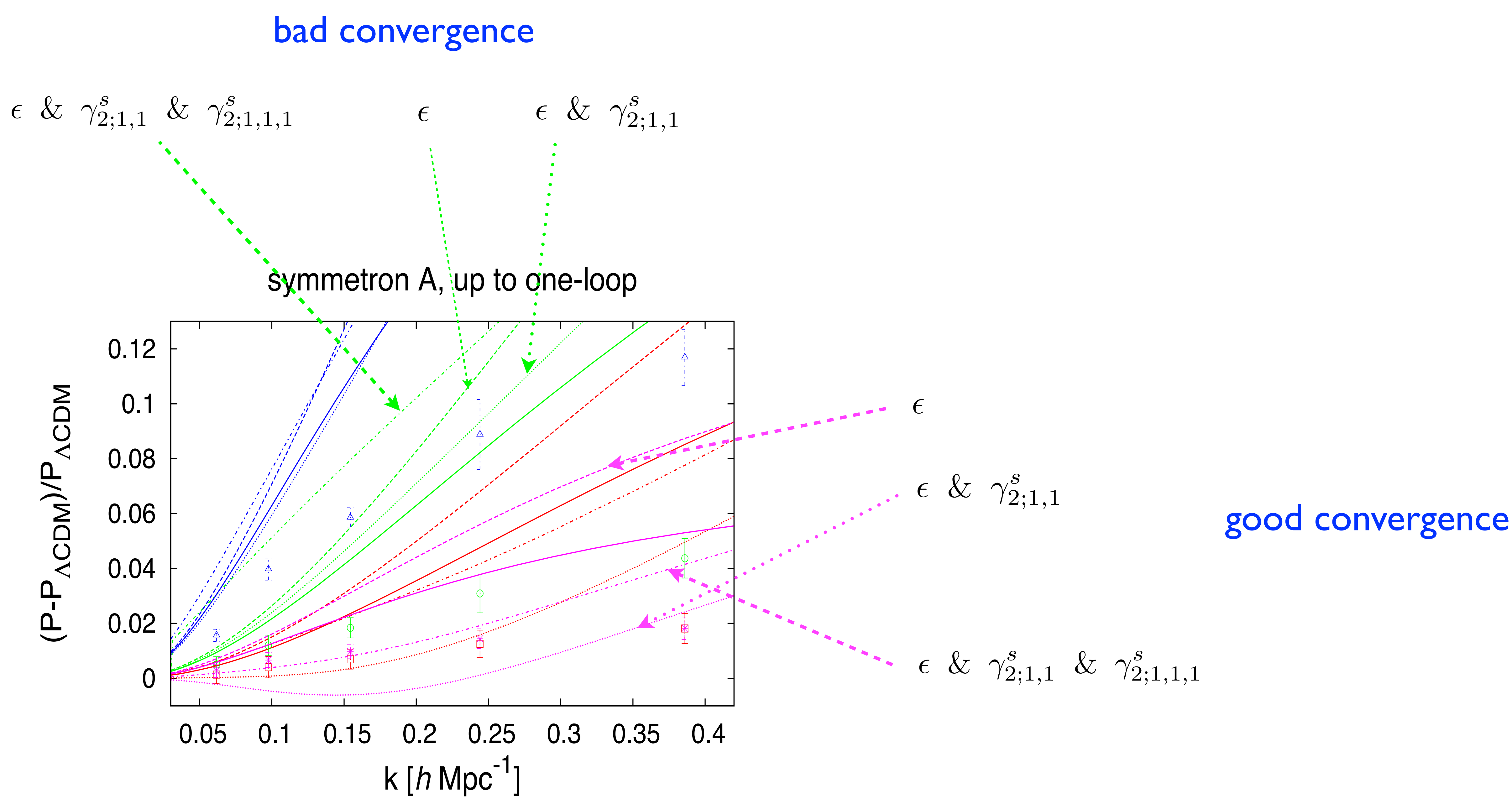

✦ For some models, going up to the cubic vertex can degrade the analytical predictions !

➡ bad convergence of higher orders

✦ This corresponds to models where the coupling functions are singular.

$$\beta(a) = \beta_0 \left[1 - \left(\frac{a_s}{a}\right)^3\right]^{\hat{n}} \qquad m(a) = m_0 \left[1 - \left(\frac{a_s}{a}\right)^3\right]^{\hat{m}} \qquad \hat{n} = 0.25, \quad \hat{m} = 0.5$$

Spherical collapse

To go beyond 1-loop standard perturbation theory, we wish to combine the perturbative expansion with a halo model. We need to take into account the impact of modified gravity on the halo mass function

→ study how the spherical collapse is modified

5th force: $\ddot{r} = -\frac{\partial \Psi_N}{\partial r} - \frac{\partial \Psi_A}{\partial r}$ (for f(R) and dilaton models)

normalized radius y(t): $y(t) = \frac{r(t)}{a(t) q} \quad \text{with} \quad q = \left(\frac{3M}{4\pi \bar{\rho}_0} \right)^{1/3}, \quad y(t=0) = 1$ $\delta(< r) = y^{-3} - 1$

$$\boxed{\frac{\partial^2 y}{\partial \eta^2} + \frac{1 - 3w\Omega_{\rm de}}{2} \frac{\partial y}{\partial \eta} + \frac{\Omega_m}{2} \left(y^{-3} - 1 \right) y = \frac{-3\Omega_m y}{8\pi \mathcal{G} \bar{\rho} r} \frac{\partial \Psi_A}{\partial r}}$$

in GR, all shells evolve independently before shell crossing

the 5th force depends on the profile

→ all shells are coupled

Simplifying approximation: use an ansatz for the density profile, parameterized by the density contrast of the mass-shell of interest:

typical profile of rare events (neglecting nonlinear distortions)

$$\delta(x) = \frac{\delta_M}{\sigma_{x_M}^2} \int_{V_M} \frac{d\mathbf{x}'}{V_M} \, \xi_L(\mathbf{x}, \mathbf{x}')$$

a) f(R) models

Normalized fluctuation of the Ricci scalar: $\delta R = 8\pi\mathcal{G}\bar{\rho}\,\alpha(x)$

eq. of motion for the shell M:

$$\frac{d^2 y_M}{d\eta^2} + \frac{1-3w\Omega_{\rm de}}{2}\frac{dy_M}{d\eta} + \frac{\Omega_m}{2}\left(y_M^{-3}-1\right)y_M = \frac{-\Omega_m y_M}{2}\int_0^{x_M}\frac{dx\,x^2}{x_M^3}(\delta-\alpha)$$

constraint eq. for the new field:

$$\frac{d^2\alpha}{dx^2} + \frac{2}{x}\frac{d\alpha}{dx} - \frac{(n+2)\Omega_{m0}}{\Omega_{m0}(1+\alpha)+4\Omega_{\Lambda 0}a^{-3}}\left(\frac{d\alpha}{dx}\right)^2 = a^2 m_0^2\left(\frac{\Omega_{m0}a^{-3}(1+\alpha)+4\Omega_{\Lambda 0}}{\Omega_{m0}+4\Omega_{\Lambda 0}}\right)^{n+2}(\alpha-\delta)$$

- Large scales: weak-field (linear) regime, $\frac{d}{dx}\to 0,\quad \alpha\to\delta$ ⇨ GR
- High density: strong-field (nonlinear) regime, $\delta\to\infty,\quad \alpha\to\delta$ ⇨ GR

⇨ chameleon mechanism due to the nonlinearity.

Because of the 5th force, the linear density threshold to reach a given nonlinear density contrast (200) is smaller than for LCDM.

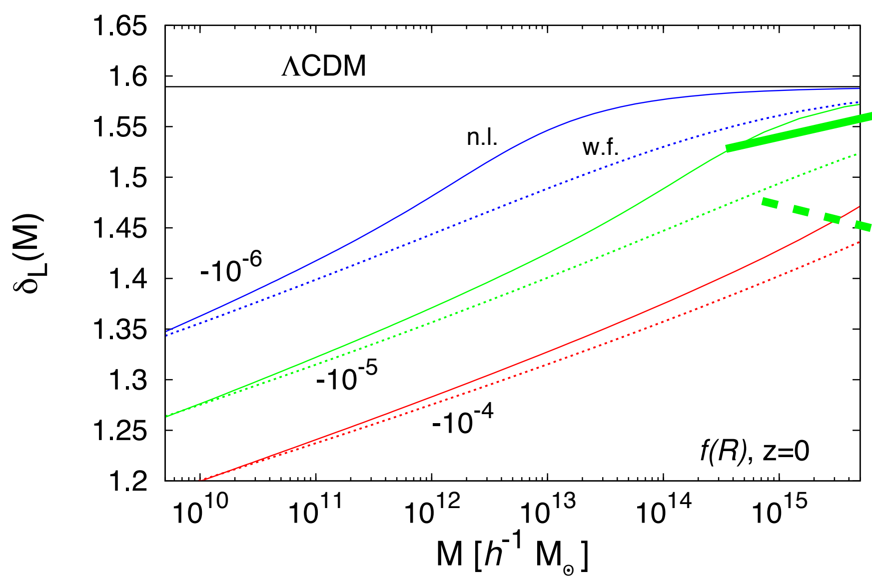

nonlinear chameleon mechanism

weak-field (linear) approximation

FIG. 6: Linear density threshold $\delta_L(M)$, associated with a nonlinear density contrast $\delta = 200$, for $f(R)$ theories at $z = 0$. The dotted lines (w.f.) correspond to the weak-field limit (108) and the solid lines (n.l.) to the fully nonlinear constraint (106).

Chameleon effect is greater for large masses, where nonlinearities can overcome spatial gradients.

✦ The linear density threshold becomes mass-dependent: $\delta_L(M)$

✦ The deviation from LCDM diminishes at high mass.

✦ The nonlinear chameleon effect decreases the deviation from LCDM. It is more efficient for large masses.

b) Scalar field models

"Normalized" scalar field: $\alpha(x) = a[\varphi(x)]$

eq. of motion for the shell M: $$\frac{d^2 y_M}{d\eta^2} + \frac{1-3w\Omega_{\rm de}}{2}\frac{dy_M}{d\eta} + \frac{\Omega_m}{2}\left(y_M^{-3}-1\right)y_M = \frac{-9\Omega_m a \beta_\alpha^2 y_M}{m_\alpha^2 \alpha^4 x_M}\frac{\partial\alpha}{\partial x}$$

Klein-Gordon eq.: $$\frac{d^2\alpha}{dx^2} + \frac{2}{x}\frac{d\alpha}{dx} + \left[\frac{d\ln\beta_\alpha}{d\alpha} - 2\frac{d\ln m_\alpha}{d\alpha} - \frac{4}{\alpha}\right]\left(\frac{d\alpha}{dx}\right)^2 = \frac{m_\alpha^2\alpha^4}{3a}\left[1+\delta-\frac{a^3}{\alpha^3}\right]$$

✦ Large scales: weak-field (linear) regime, $\frac{d}{dx} \to 0, \quad \alpha \to a(1+\delta)^{-1/3}$ ➡ GR

✦ High density: strong-field (nonlinear) regime, $\delta \to \infty, \quad \alpha \to a\delta^{-1/3}$

dilaton models: $\frac{\beta_\alpha^2}{m_{\alpha^2}} \to 0$

symmetron models: $\alpha \to a_s$

➡ GR

➡ screening mechanism due to the nonlinearity.

Because of the 5th force, the linear density threshold to reach a given nonlinear density contrast (200) is smaller than for LCDM.

dilaton models

symmetron models

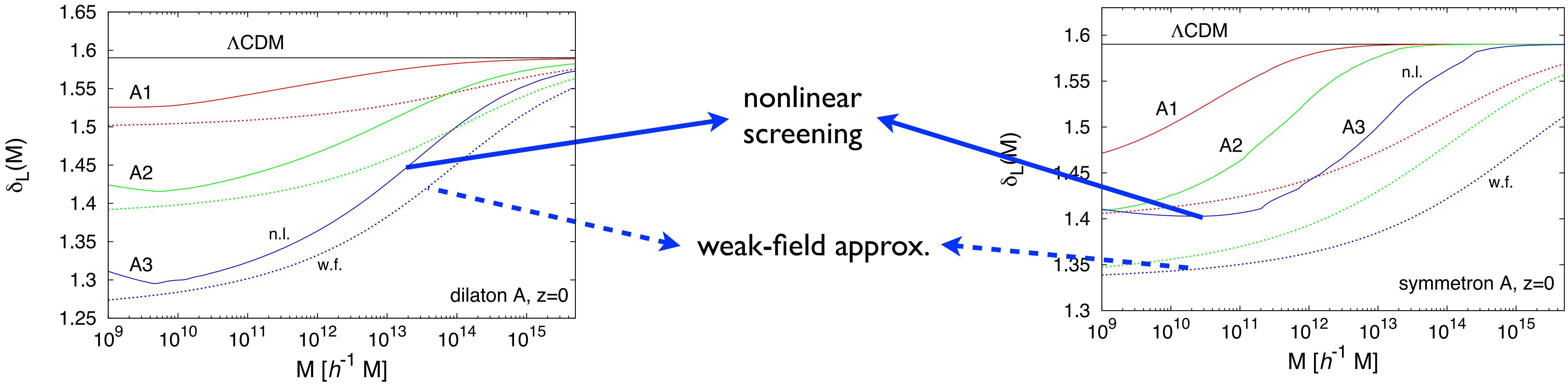

✦ Again, nonlinearities (screening) decrease the deviation from GR.

✦ The rate of convergence to GR at high mass depends on the model (very efficient for symmetron, very nonlinear models).

✦ Contrary to f(R) models, at low mass we do not converge to weak-field prediction but to GR.

c) K-mouflage models

Trajectories in physical coordinates: $$\ddot{\mathbf{r}} + \frac{d\ln\bar{A}}{dt}\dot{\mathbf{r}} - \left(\frac{\ddot{a}}{a} + \frac{\dot{a}}{a}\frac{d\ln\bar{A}}{dt}\right)\mathbf{r} = -\nabla_r(\Psi_{\rm N} + \ln A)$$

Scale-independence ➡ the motions of different mass shells are decoupled, as in LCDM (before shell-crossing)

linear density contrast threshold:

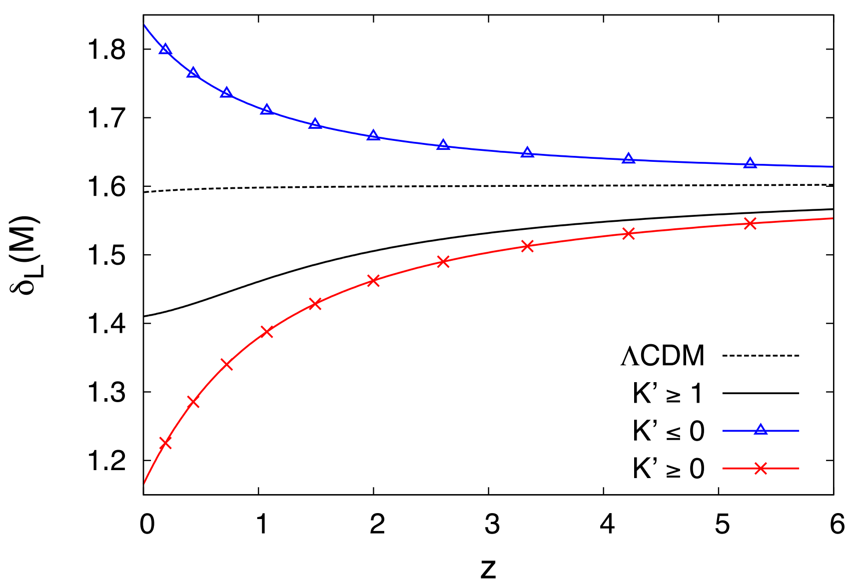

d) Halo mass function

$$M \to \infty : \quad \ln[n(M)] \sim -\frac{\delta_c(M)^2}{2\sigma(M)^2}$$ with $$\delta_c(M) = \mathcal{F}_q^{-1}(200)$$

Use the Press-Schechter scaling: $$n(M)\frac{dM}{M} = \frac{\bar{\rho}_m}{M} f(\nu)\frac{d\nu}{\nu}$$ with $$\nu = \frac{\delta_c(M)}{\sigma(M)}$$

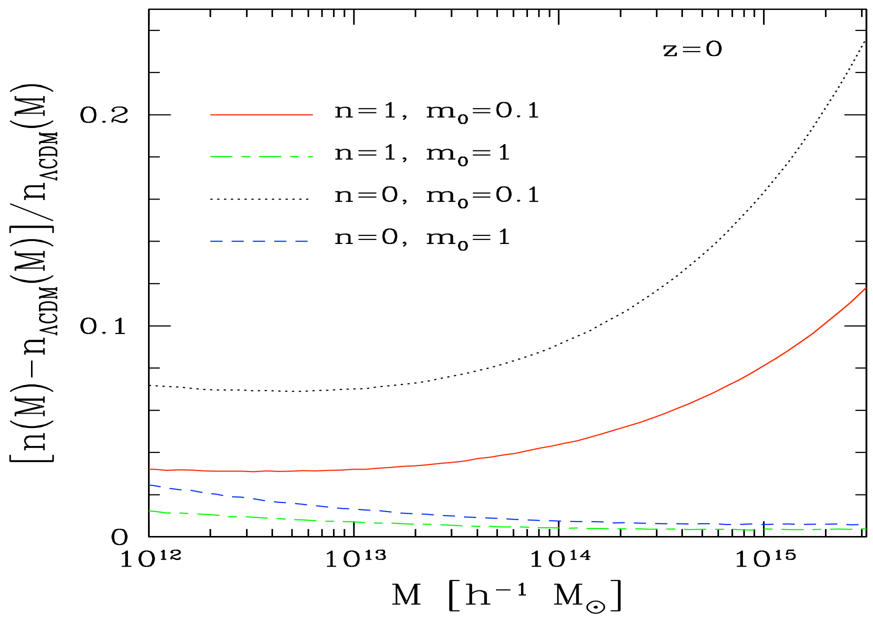

Relative deviation of the mass function

case where $\epsilon(k,a) > 0$

e) Probability distribution of the density contrast

From the spherical dynamics we can also obtain the PDF of the density contrast within spherical cells, in the weakly non-linear regime.

Introduce the cumulant generating function (Laplace transform):

$$e^{-\varphi(y)/\sigma_x^2} \equiv \langle e^{-y\delta_x/\sigma_x^2} \rangle = \int_{-1}^{\infty} d\delta_x \; e^{-y\delta_x/\sigma_x^2} \; \mathcal{P}(\delta_x)$$

$$e^{-\varphi(y)/\sigma_x^2} = (\det C_{\delta_L \delta_L}^{-1})^{1/2} \int \mathcal{D}\delta_L \; e^{-S[\delta_L]/\sigma_x^2}$$

where

$$S[\delta_L] = y\,\delta_x[\delta_L] + \frac{\sigma_x^2}{2}\,\delta_L \cdot C_{\delta_L\delta_L}^{-1} \cdot \delta_L$$

On large scales, we obtain:

$$\boxed{\sigma_x \to 0 : \quad \varphi(y) \to \min_{\delta_L} S[\delta_L]}$$

For spherical cells, we can look for the spherical minimum (saddle-point)

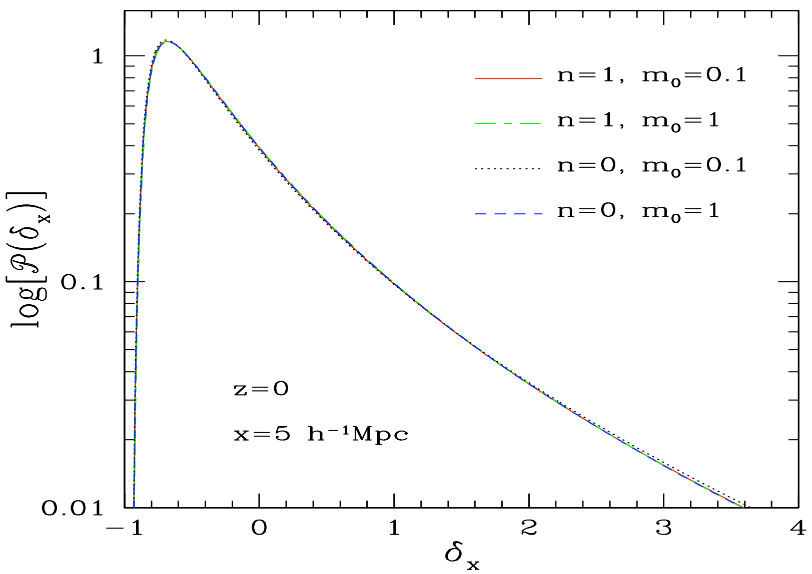

Probability distribution function

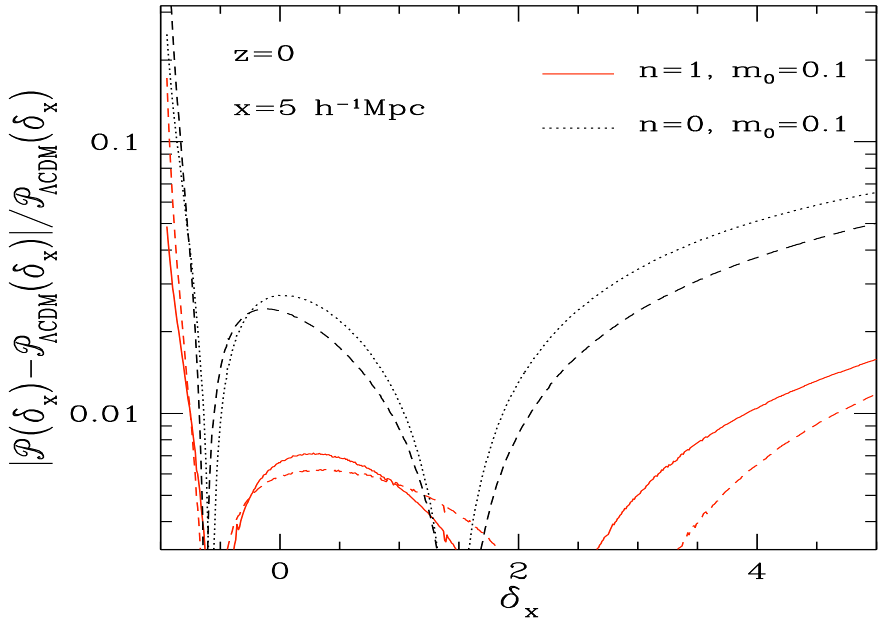

Relative deviation

case where $\epsilon(k,a) > 0$

Matter power spectrum

As in the halo model (but from a Lagrangian point of view), decompose the power spectrum as

$$P(k) = P_{2\mathrm{H}}(k) + P_{1\mathrm{H}}(k)$$

"2-halo term"

perturbative contribution

$$P_{2\mathrm{H}}(k) \simeq F_{2\mathrm{H}}(1/k)\; P_{\mathrm{pert}}(k)$$

(high-k behavior improved by going beyond standard perturbation theory)

"1-halo term"

nonperturbative contribution

$$P_{1\mathrm{H}}(k) = \int_0^\infty \frac{d\nu}{\nu}\, f(\nu)\, \frac{M}{\bar{\rho}(2\pi)^3}\, \left(\tilde{u}_M(k)^2 - \tilde{W}(k\, q_M)^2\right)$$

halo mass function

halo density profile

(low-k behavior solved by counterterm)

a) f(R) models

Relative deviation from LCDM for P(k)

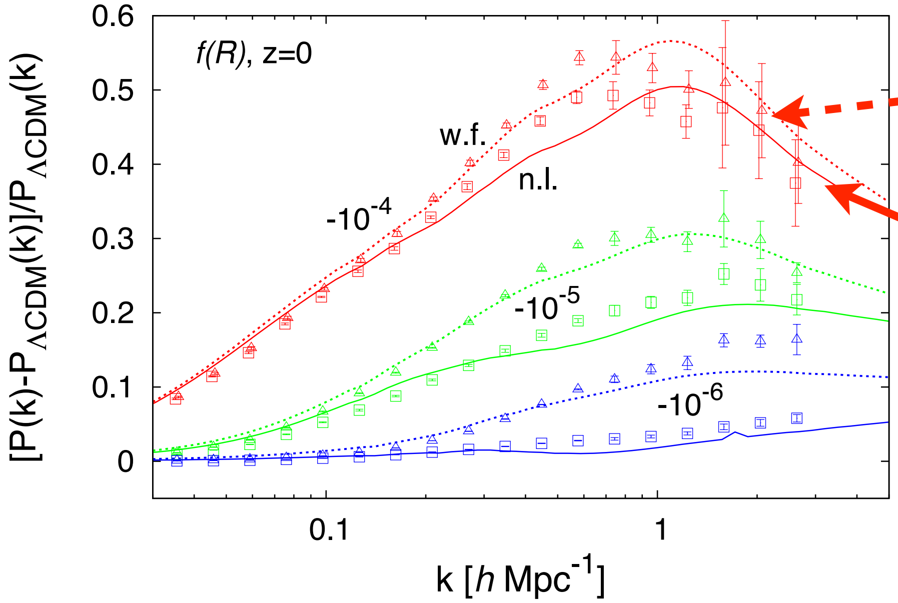

"no-chameleon" simulations △ (linear modification of gravity: ϵ)

"with-chameleon" simulations □ (nonlinear modification of gravity: ϵ, $\gamma^{s}_{i;i_1,..,i_n}$)

FIG. 13: Relative deviation from Λ-CDM of the power spectrum in $f(R)$ theories, at redshift $z = 0$, for $n = 1$ and $f_{R_0} = -10^{-4}, -10^{-5}$, and -10^{-6}. In each case, the triangles and the squares are the results of the "no-chameleon" and "with-chameleon" simulations from [25], respectively. We plot the relative deviation of the nonlinear power power spectrum without chameleon effect (w.f., dotted lines) and with chameleon effect (n.l., solid lines).

✦ Reasonably good agreement between simulations and analytical predictions, from linear to mildly nonlinear scales.

✦ As compared with parameterizations (PPF), the convergence to GR on small scales is not put by hand. It is due to the chameleon mechanism.

b) Scalar field models

Relative deviation from LCDM for P(k)

no screening, only ϵ

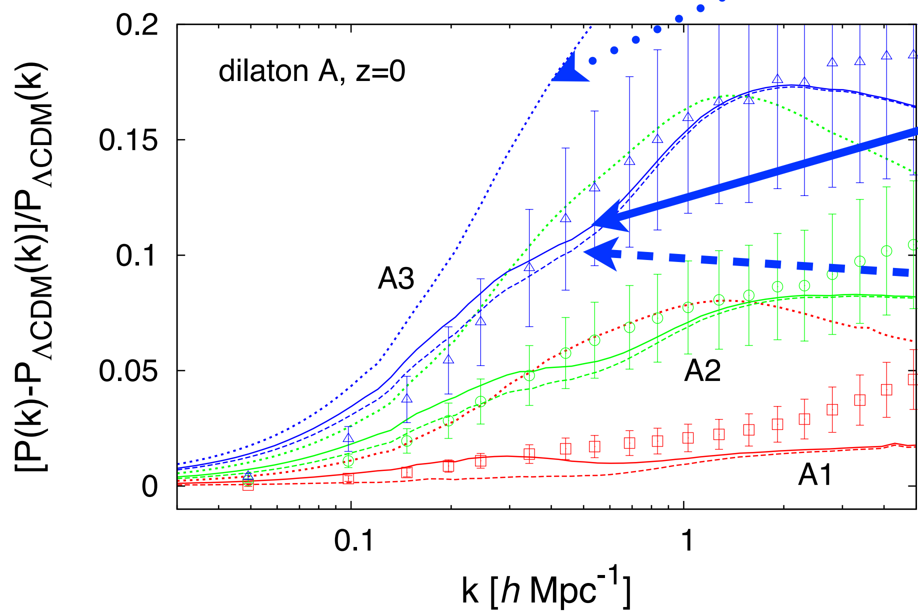

screening, one-loop with quadratic & cubic vertices $\gamma^s_{2;1,1}$ & $\gamma^s_{2;1,1,1}$

screening, one-loop with quadratic vertex $\gamma^s_{2;1,1}$

- ✦ The impact of the nonlinear screening mechanism is greater than for the f(R) models.
- ✦ Reasonably good agreement with simulations.
- ✦ Underestimate at high k, could be due to the neglect of halo profile modifications.

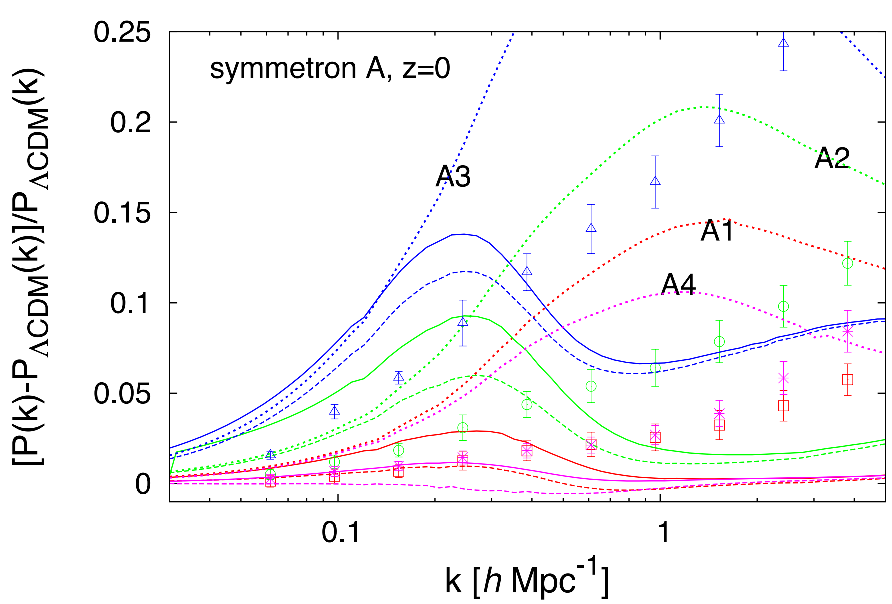

Bad convergence, but we can guess beforehand the problematic cases.

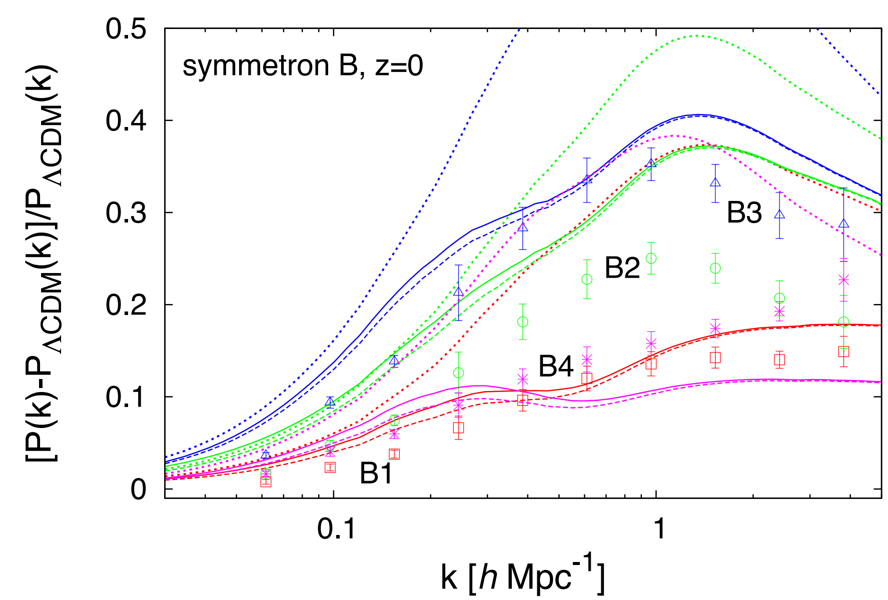

Good convergence, reasonable agreement.

Conclusion

✦ "Modified-gravity" models introduce a new degree of freedom (new field).

✦ Using the quasi-static approximation, we can go back to the standard framework, defined by the matter density and velocity fields, with a modified "gravitational" potential.

✦ "Standard" perturbation theory can be generalized in a direct manner. The main differences are:

- new complex time and scale dependences.
- new nonlinear vertices (the eqs. of motion are no longer quadratic), which are the first signs of nonlinear screening mechanisms.

✦ The spherical collapse is more complex, because of the coupling between different shells. Nevertheless, this can be simplified using approximate density profiles.

✦ Explicit account of nonlinear chameleon or screening mechanisms that ensure convergence to GR in high-density environments.

✦ By combining perturbation theory and halo model (spherical collapse), one can obtain reasonably good predictions up to mildly nonlinear scales, for models that are not too singular.

✦ Singular models lead to bad convergence of perturbative expansions and low accuracy of analytical predictions. Fortunately, these cases can be detected before hand.

✦ To handle difficult cases, or to go beyond the quasi-static approximation, one may need to explicitly keep track of the new scalar field in the perturbative approach ?

Supplements

P.V., T. Nishimichi, A. Taruya (2013)

Matter density power spectrum:

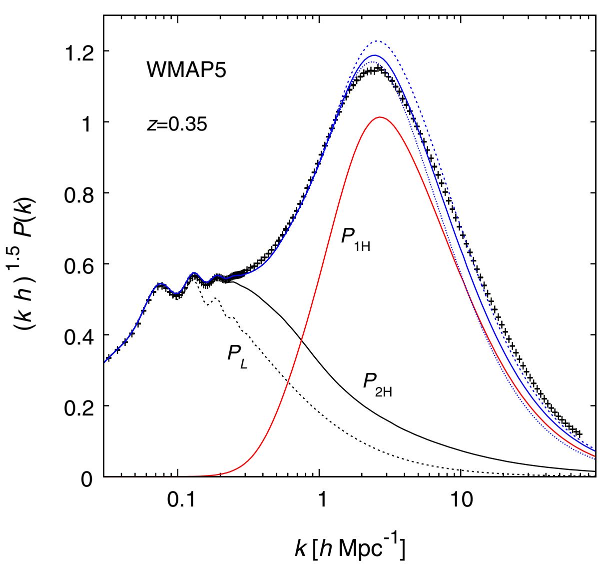

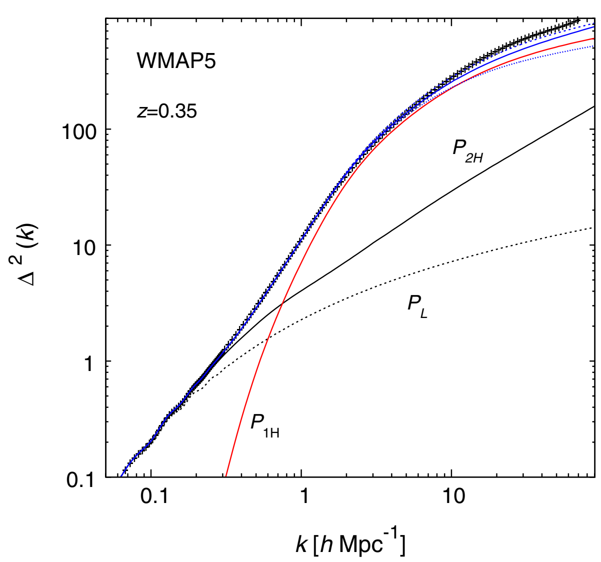

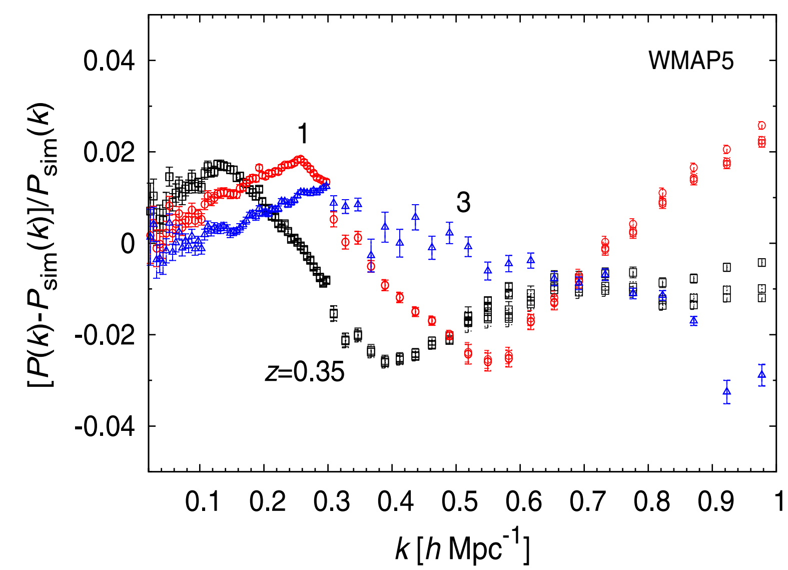

Matter density correlation function:

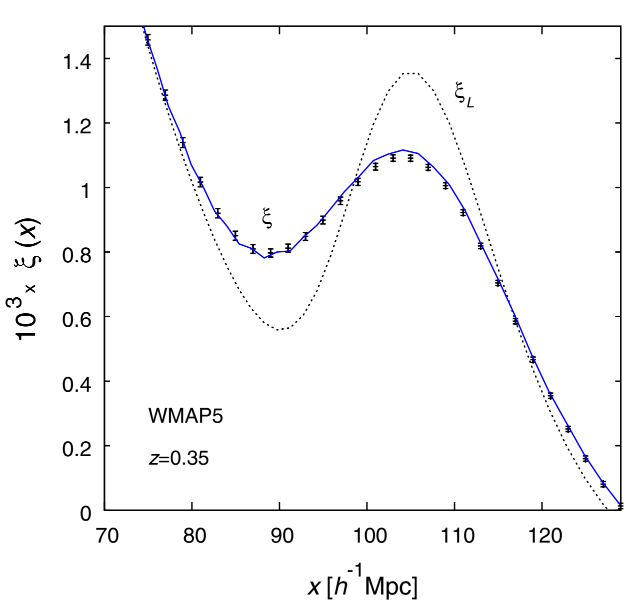

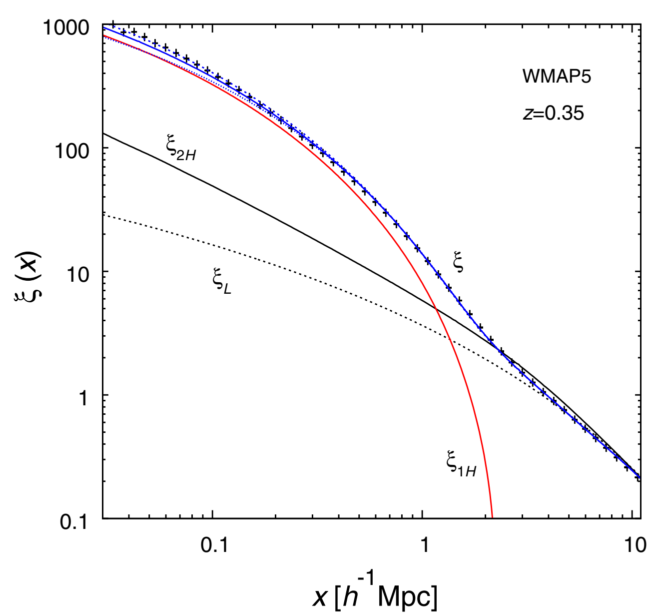

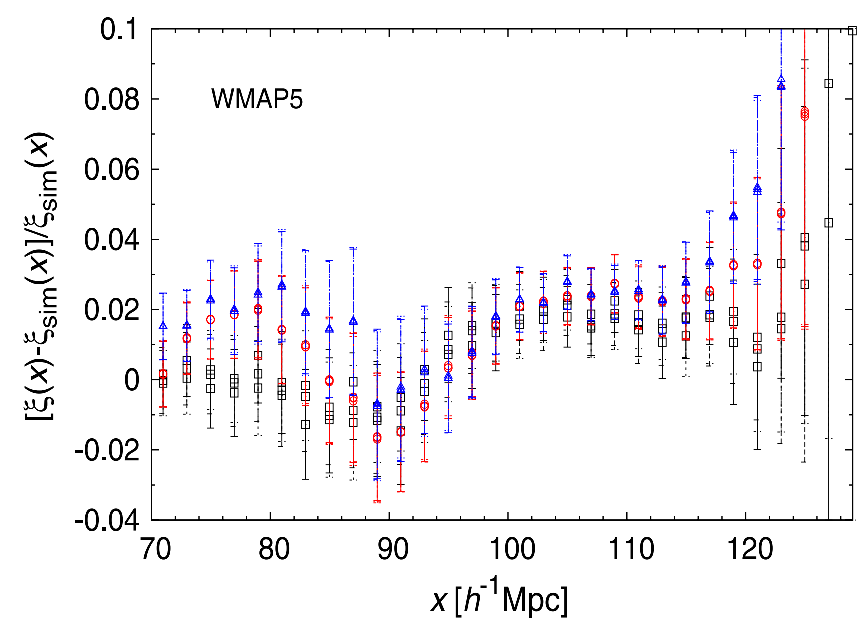

BAO scales

power spectrum

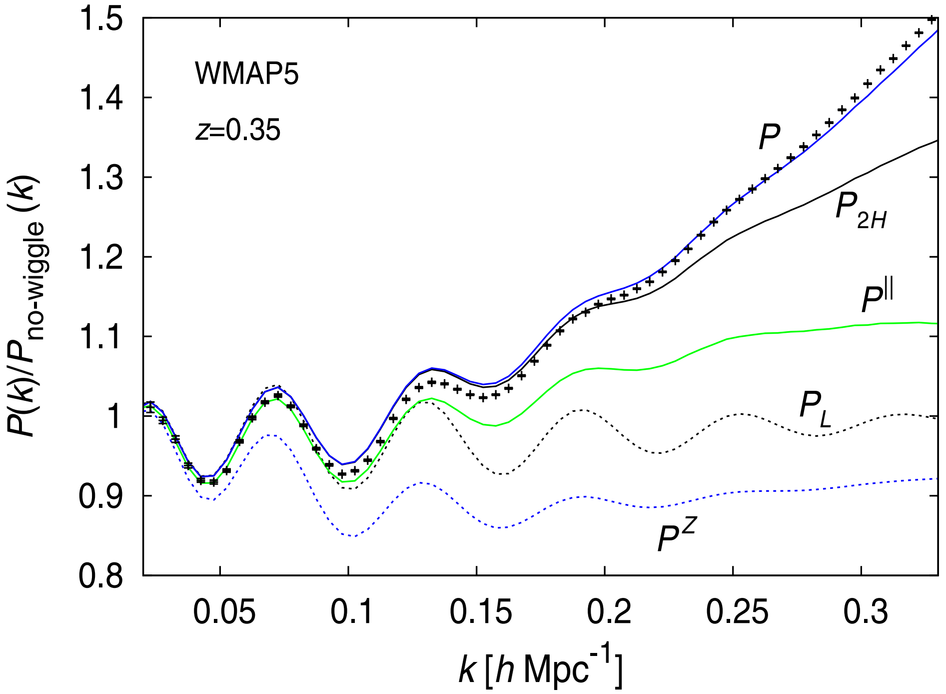

correlation function